

Ultrasound modulated optical tomography contrast enhancement with non-linear oscillation of microbubbles

Haowen Ruan^{1,2}, Melissa L. Mather^{1,3}, Stephen P. Morgan¹

¹Electrical Systems and Optics Research Division, Faculty of Engineering, University of Nottingham, Nottingham, NG7 2RD, UK; ²Department of Electrical Engineering, California Institute of Technology, 1200 E California Boulevard, Pasadena, California 91125, USA; ³Institute of Biophysics, Imaging and Optical Sciences, University of Nottingham, UK

Correspondence to: Stephen P. Morgan. Head of Electrical Systems and Optics Research Division, Prof. of Biomedical Engineering, Faculty of Engineering, University of Nottingham, NG7 2RD, UK. Email: steve.morgan@nottingham.ac.uk.

Background: Ultrasound modulated optical tomography (USMOT) is an imaging technique used to provide optical functional information inside highly scattering biological tissue. One of the challenges facing this technique is the low image contrast.

Methods: A contrast enhancement imaging technique based on the non-linear oscillation of microbubbles is demonstrated to improve image contrast. The ultrasound modulated signal was detected using a laser pulse based speckle contrast detection system. Better understanding of the effects of microbubbles on the optical signals was achieved through simultaneous measurement of the ultrasound scattered by the microbubbles.

Results: The length of the laser pulse was found to affect the system response of the speckle contrast method with shorter pulses suppressing the fundamental ultrasound modulated optical signal. Using this property, image contrast can be enhanced by detection of the higher harmonic ultrasound modulated optical signals due to nonlinear oscillation and destruction of the microbubbles. Experimental investigations were carried out to demonstrate a doubling in contrast by imaging a scattering phantom containing an embedded silicone tube with microbubbles flowing through it.

Conclusions: The contrast enhancement in USMOT resulting from the use of ultrasound microbubbles has been demonstrated. Destruction of the microbubbles was shown to be the dominant effect leading to contrast improvement as shown by simultaneously detecting the ultrasound and speckle contrast signals. Line scans of a microbubble filled silicone tube embedded in a scattering phantom demonstrated experimentally the significant image contrast improvement that can be achieved using microbubbles and demonstrates the potential as a future clinical imaging tool.

Keywords: Ultrasound modulated optical tomography (USMOT); microbubbles; optical scattering; harmonic imaging; ultrasound

Submitted Oct 09, 2014. Accepted for publication Oct 20, 2014.

doi: 10.3978/j.issn.2223-4292.2014.11.30

View this article at: <http://dx.doi.org/10.3978/j.issn.2223-4292.2014.11.30>

Introduction

Imaging inside optically scattering media such as tissue is challenging using optical techniques alone. By detecting light modulated by ultrasound, ultrasound modulated optical tomography (USMOT) is able to provide optical spatial resolution comparable to ultrasound imaging and offers the potential for quantitative functional imaging in tissue.

However, the ultrasound modulated light is often very weak compared with the background unmodulated light resulting in a low signal to noise ratio (SNR) and low contrast images. Parallel speckle detection techniques (1,2) were proposed to improve the SNR as a large optical acceptance angle can be obtained. Holography technique based on a photorefractive medium (3) and a photo detector array (4,5)

further improved the SNR as optical gain of the ultrasound modulated signal was achieved through interference with a reference beam. Recently, a wavefront shaping technique (6-8) was used to enhance light at the focus of the ultrasound so that imaging contrast can be improved. The SNR improvement using all these techniques was achieved by improving the optical detection of the system.

Another approach to improve the contrast of the USMOT image lies in optimising the ultrasound propagation such as reducing the effect of shear wave modulated light (9), using the acoustic radiation force (10) and detecting the second harmonic ultrasound modulated signal arising from non-linear propagation (5,11-13) and bubble oscillation. Nonlinear ultrasound in general has been widely used to enhance the contrast of ultrasound imaging. To further improve the contrast in conventional ultrasound imaging, microbubbles are often applied to the imaging target to enhance the acoustic wave reflectivity (14). There are a number of different mechanisms that give rise to enhanced image contrast using microbubbles. Depending on the ultrasound power, microbubbles can be used to produce images based on detection of the fundamental frequency, the second harmonic, arising predominantly from non-linear bubble oscillation, and transient broadband ultrasound emission due to destruction of the bubbles (14). In particular, detection of the second harmonic signal arising from non-linear oscillation is useful as the nonlinear signal generation is much stronger from the microbubbles than the surrounding tissue. Pulse inversion is one of the techniques that is typically used in second harmonic detection as it enables the fundamental frequency to be suppressed (15). In relation to USMOT, microbubbles can be used to increase the magnitude of the ultrasound modulated optical signal. This has been studied both theoretically (16) and experimentally (17) but to date only the ultrasound modulation at the fundamental frequency has been considered. The observed signal enhancements arise due to the large differences in the acoustic impedance of microbubbles compared to the surrounding tissue. Here we demonstrate a speckle contrast detection technique in which the fundamental ultrasound modulated signal is suppressed while higher harmonic signals remain or are less suppressed. Distinct to the speckle contrast technique described previously (18), in this work a pulsed laser light modulated by an ultrasound tone burst is used that allows the system to achieve a high pass filter response. Results demonstrate that the suppression of the fundamental frequency by the high pass filter provides enhanced image contrast.

Methods

Experiment

The experimental setup is shown in *Figure 1*. One channel of a software-triggered dual channel function generator (Tektronix AFG3022B, function generator A) was used to produce 2.25 MHz tone bursts of 1 ms duration with a duty cycle that was altered depending on the required frequency response of the detection system. This signal was then amplified by a power amplifier (Amplifier Research 75A250A) and used to drive the transmitting ultrasound transducer (Olympus A304S, 2.25 MHz, 48 mm focal length). The second channel of function generator A produced pulsed signals of the same frequency and overall duration as the first. These pulses were used to trigger function generator B (Tektronix AFG3252) which generated 80 MHz burst signals for the acousto-optic modulator (AOM, Isomet 1205c-1) that modulated a continuous wave (CW) laser (Oxxius Slim 50 mW, 532 nm wavelength). The AOM acts as a shutter for the illumination by selecting the first order of the diffracted light using an aperture which allowed the illuminating laser pulses to be synchronised with the ultrasound signal. The laser pulses were then modulated by the ultrasound wave inside the scattering medium resulting in ultrasound modulated light which was detected by a CCD camera (Hamamatsu ORCA C4742-95-12ERG, 1,344×1,024 pixels, 12 bits, pixel size 6.45 μm by 6.45 μm). A second aperture was placed in front of the camera to control the speckle size so that speckle contrast was maximized [the speckle correlation area is sampled by four pixels (19)]. A silicone tube (3 mm inner diameter, 0.75 mm wall thickness) was embedded in a scattering phantom and connected to a computer controlled syringe pump to control the flow of microbubbles (Optison, GE Healthcare) through the silicone tube. The silicone tube was tilted by $\sim 15^\circ$ to the z axis so that incident light can uniformly illuminate the sample. The microbubbles had a nominal size of 3.0–4.5 μm and were used at a concentration of 0.2% v/v. During measurement the syringe pump was switched off and was switched on to refresh the bubbles between measurements. A second ultrasound transducer (Olympus V307, 5 MHz, 50 mm focal length, 0.6 mm calculated -6 dB beam diameter, 8.8 mm calculated -6 dB focal zone) was used as a receiver to detect the ultrasound scattered from the sample. The detected ultrasound signal was amplified (Stanford Research Systems, SR445A) and then recorded by an oscilloscope (Tektronix, DPO2024). Both the camera and oscilloscope were triggered by the

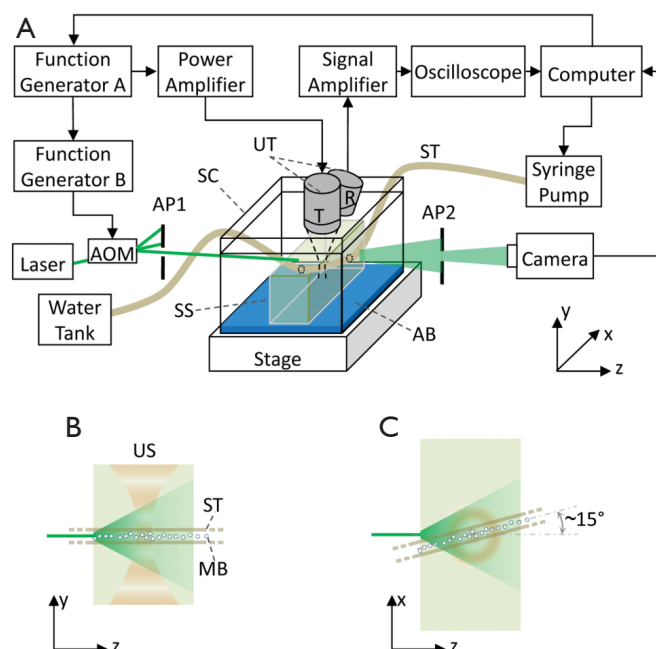


Figure 1 Experimental setup. (A) The system simultaneously detects the ultrasound reflected from the sample and ultrasound modulated optical signal. The AOM acts as a shutter which converts the CW laser to a laser pulse train with the same repetition rate as the ultrasound signal. Transducer T generates a tone burst ultrasound signal which modulates the scattered light inside the scattering phantom. Transducer R receives the scattered signals from the tube which is centred at the focal zone of the transducer. The camera detects the light from the scattering phantom. (B) y - z view and (C) x - z view of the sample structure. The ultrasound focuses on the microbubble-filled silicone tube which is embedded in the scattering sample. Abbreviations: AB, ultrasound absorber; AP, aperture; MB, microbubble; SC, sample container; SS, scattering sample; ST, silicone tube; US, ultrasound; UT, ultrasound transducer; AOM, acousto-optic modulator; CW, continuous wave.

function generators. This experimental setup enables the speckle contrast and scattered ultrasound signal to be measured simultaneously.

The background sample used in this experiment was a scattering phantom ($x=90$ mm, $y=50$ mm, $z=15$ mm) made of agarose and polystyrene microspheres resulting in a scattering coefficient of 2.3 mm^{-1} ($g=0.932$). The liquid sample that flowed through the silicone tube was prepared using the same polystyrene microspheres ($1.6 \mu\text{m}$) and water and therefore had a similar scattering coefficient as the background sample. Two ultrasound transducers focused on the silicone tube at the mid-plane (x, y) of the phantom at a common point. The computer controlled function generator triggered ultrasound (~ 1 ms duration) and the digital oscilloscope. After a time delay ($40 \mu\text{s}$) allowing for propagation of the US pulse to the focal region, the laser pulse duration (1 ms) and the camera (1 ms exposure time) were triggered simultaneously. A comparison between results obtained with and without microbubbles was carried out. The microbubble concentration used was 0.2% v/v.

The ultrasound pressure at the focal point was 480 kPa (measured with a 0.2 mm calibrated needle hydrophone, Precision Acoustics), resulting in a mechanical index (MI) of 0.32. The MI is lower than the ultrasound safety threshold (MI = 0.4) for tissue containing a gas body (20).

Speckle processing

An optical speckle contrast detection technique (21) was used to analyse the ultrasound modulated optical signal in which speckle contrast is measured in two separate frames with the ultrasound on and off. The ultrasound modulated signals (AC) are averaged out over the integration time of the camera resulting in a decrease in speckle contrast whereas contrast is retained for a static speckle pattern (DC). A signal mixing approach can be used to shift the AC signals to DC and attenuate the signal from a certain frequency band. In this case, pulsed laser illumination is used rather than CW as described in (21). In order to image non-linear ultrasound modulated signals, the fundamental

was suppressed by using ultrasound to modulate a laser pulse train whose pulse repetition rate equals the ultrasound frequency. Let $I(t)$ be the light intensity on each pixel of the camera if the laser intensity were kept constant

$$I(t) = I_{dc} + I_{ac} + 2\sqrt{I_{dc}I_{ac}} \cos(2\pi ft + \varphi) \quad [1]$$

where I_{dc} and I_{ac} are the amplitudes of the DC and AC light intensity respectively; f is the frequency of the ultrasound; φ is the random phase of the speckle. The modulation function of the laser pulse train is given in Fourier series,

$$D(t) = \frac{a}{b} + \sum_{n=1}^{\infty} A_n \cos(2\pi f_0 n t) \quad [2]$$

where $A_n = \frac{2}{n\pi} \sin\left(\frac{2\pi f_0 n a}{2}\right)$ is the Fourier coefficient; $\frac{a}{b}$ and f_0

is the duty cycle and fundamental frequency of the laser pulse train respectively. Therefore, the time-averaging intensity of the ultrasound modulated laser pulse train on the i^{th} pixel is given by

$$I = \frac{1}{T_e} \int_0^{T_e} I(t)D(t)dt \quad [3]$$

Substituting $I(t)$ and $D(t)$ in Eq. [3], expanding the series and then neglecting the terms with $f_0 T_e (>> 1)$ in the denominator, gives;

$$I \approx I'_{dc} + I'_{ac} + 2\sqrt{I'_{dc}I'_{ac}} \text{sinc}\left(\frac{fT_e}{2}\right) \cos(\pi f T_e + \varphi) + \sqrt{I'_{dc}I'_{ac}} \frac{b}{a} \sum_{n=1}^{\infty} A_n \text{sinc}\left(\frac{nf_0 T_e - fT_e}{2}\right) \cos(n\pi f_0 T_e - \pi f T_e + \varphi) \quad [4]$$

where $I'_{dc} = I_{dc} \frac{a}{b}$ and $I'_{ac} = I_{ac} \frac{a}{b}$ is the mean light intensity of DC and AC light respectively. The speckle contrast is given by

$$C = \frac{\sqrt{\langle I^2 \rangle} - \langle I \rangle^2}{\langle I'_{dc} \rangle + \langle I'_{ac} \rangle} \quad [5]$$

Substituting Eq. [4], into Eq. [5], the equation can be further simplified by retaining the first two terms of the Taylor series;

$$C_{dc} + \frac{M}{C_{dc}} \left[\text{sinc}^2\left(\frac{fT_e}{2}\right) + \frac{1}{4} \left(\frac{b}{a}\right)^2 \sum_{n=1}^{\infty} A_n^2 \text{sinc}^2\left(\frac{f_0 n T_e - fT_e}{2}\right) \right] \quad [6]$$

$$C \approx \frac{C_{dc} + \frac{M}{C_{dc}} \left[\text{sinc}^2\left(\frac{fT_e}{2}\right) + \frac{1}{4} \left(\frac{b}{a}\right)^2 \sum_{n=1}^{\infty} A_n^2 \text{sinc}^2\left(\frac{f_0 n T_e - fT_e}{2}\right) \right]}{1 + M}$$

where $M = \frac{I'_{ac}}{I'_{dc}}$ is defined as the modulation depth,

$$C_{dc} = \frac{\sqrt{\langle I'_{dc}{}^2 \rangle} - \langle I'_{dc} \rangle^2}{\langle I'_{dc} \rangle}$$

is the speckle contrast of the DC signal.

The terms within the square brackets in Eq. [6] describe the Fourier power spectrum of the laser pulse train $D(t)$. This power spectrum can be denoted by $S(f)$ and expressed

as:

$$S(f) = |\hat{D}(f)|^2 \quad [7]$$

where $\hat{D}(f)$ is the Fourier transform of $D(t)$.

In the experiments, the speckle contrast difference between ultrasound off and on is considered as the ultrasound modulated signal which is given by

$$C_{diff} = C_{dc} - C \quad [8]$$

Substituting Eq. [6] and the expression for C_{dc} into Eq. [8];

$$C_{diff} \approx \frac{MC_{dc} - \frac{M}{C_{dc}} S(f)}{1 + M} \quad [9]$$

For a fully developed speckle pattern, the speckle contrast of the static optical signal is 1 (22) ($C_{dc}=1$). Therefore, Eq. [9] can be further reduced to

$$C_{diff} \approx \frac{M}{1 + M} [1 - S(f)] \quad [10]$$

From the above it can be seen that the frequency response of the detection system can be controlled by tuning the parameters (i.e., duty cycle) of the laser pulse train. Thus, this approach enables optimised detection of a specific frequency band of interest in the ultrasound modulated signal.

Results

In order to compare the spectrum of the ultrasound signals reflected from the microbubbles and the pass band of the system, the ultrasound signal reflected from microbubbles (0.2% v/v) was measured with its spectrum shown in *Figure 2A*. Based on Eq. [10], the system pass band can be calculated by normalizing the contrast difference over a range of frequencies. *Figure 2B-D* show the pass band of the optical detection system with speckle contrast detection using laser pulses of duty cycle at 100%, 50% and 34% respectively at a pulse repetition frequency of 2.25 MHz. It can be seen that the laser pulse train creates a notch filter which is an inverted frequency spectrum of the laser pulse train. The stop-bandwidth of each notch is determined by the camera exposure time and the envelope is determined by the laser pulse duration. Accordingly, the fundamental ultrasound modulated signal can be suppressed by using a laser pulse train with appropriate pulse duration.

In the CW laser speckle contrast method (21) signals over the entire bandwidth contribute evenly to the decrease in speckle contrast (*Figure 2B*). When pulsed light is used the fundamental ultrasound modulated signal is suppressed while the harmonic ultrasound modulated signal due to non-linear oscillation of the ultrasound microbubbles is maintained or

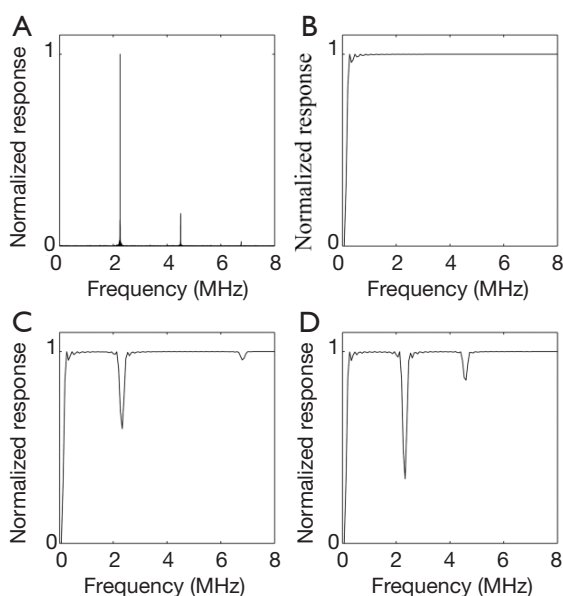


Figure 2 (A) spectrum of the ultrasound signal reflected from the microbubbles; (B-D) pass band of the speckle contrast detection with laser pulse train of 100%, 50% and 34% duty cycle respectively.

is less heavily attenuated (depending on the duty of the laser pulse train). This is a beneficial response when microbubbles that oscillate non-linearly are used as contrast agents.

The ultrasound signal reflected from the silicone tube containing the bubbles was recorded in the time domain (~1 ms). A fast Fourier transform (FFT) was then applied to the time domain ultrasound signal and a 100 kHz square window centred at the second harmonic (4.5 MHz) was used to extract the signal amplitude at the second harmonic by integration. The sample was exposed 30 times to 1 ms bursts of ultrasound and light with a 2 s time interval between exposures. To detect the ultrasound modulated optical signal with the fundamental frequency suppressed, the laser pulse train (34% duty cycle) was used as it produced a filter that significantly suppressed the fundamental component (Figure 2D). During this process, the liquid sample was not flowing (i.e., the syringe pump was off and only Brownian motion of the liquid in the tube was present).

Figure 3A shows the second harmonic ultrasound signal over the sequence of exposures in the cases of without microbubbles and with microbubbles detected by the receiving ultrasound transducer. The results show that the second harmonic signal without microbubbles is lower but constant over the exposure sequence. With microbubbles, the strength of the detected second harmonic signal decays

rapidly indicating that many of the microbubbles were destroyed following the first few exposures. However, the reflected second harmonic signal became constant after ~10 exposures and was still higher than that without microbubbles. This indicates that some bubbles remained intact in the ultrasound focal zone.

Figure 3B shows the optical speckle contrast difference, which is a measure of modulated optical signal, over the exposure sequence. A decay of the speckle contrast difference is observed for the microbubble case while it remained constant without bubbles. When microbubbles were used the ultrasound modulated optical signal enhancement can be clearly observed during the first exposure. As the exposure sequence continues, no significant enhancement is observed, although intact bubbles remained (Figure 3A). This is because the fundamental signal contribution dominated the speckle contrast difference even though it was suppressed by using the laser pulse train.

To further investigate whether the broadband acoustic emission due to destruction of the microbubbles dominates the contrast improvement, the sample with microbubbles was first exposed to low pressure ultrasound (480 kPa) under the same conditions as in Figure 3. It was then exposed to high pressure ultrasound (1.6 MPa) 30 times, and finally to low pressure ultrasound again without replenishing the bubbles. Figure 4A,B show the results of ultrasound signal and optical speckle contrast difference respectively. The decay curves of the first group of 30 exposures demonstrate the partial destruction of microbubbles [Figure 4A,B (I)]. In the second group of exposures, high pressure ultrasound caused the remaining microbubbles to be destroyed resulting in strong higher harmonic ultrasound emission. This can also be observed in the ultrasound modulated optical signal [Figure 4B (II)]. After high pressure exposure, no enhanced higher harmonic emission is observed from both ultrasound signal and ultrasound modulated optical signal [Figure 4A,B (III)].

In order to quantify the ultrasound modulated signal enhancement with microbubbles over the laser pulse duty cycle, the optical speckle contrast difference (modulated signal intensity) was measured with and without microbubbles over the laser pulse duty cycle (Figure 5A, blue). Each data point is an average of 20 measurements of speckle contrast difference with the liquid sample being refreshed before each measurement by stepping the syringe pump. The signal enhancement with microbubbles can be observed at all measurement points. The signal enhancement ratio, which is defined as the difference between signals

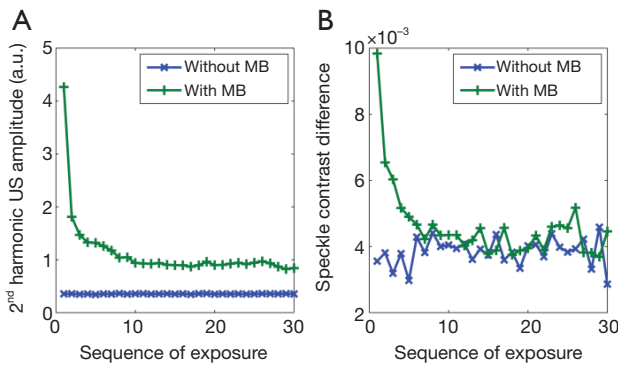


Figure 3 (A) Scattered 2nd harmonic ultrasound signal from the tube that is centred at the focal zone of the transducers; (B) optical speckle contrast difference between ultrasound on and off with fundamental frequency suppressed. MB, microbubble.

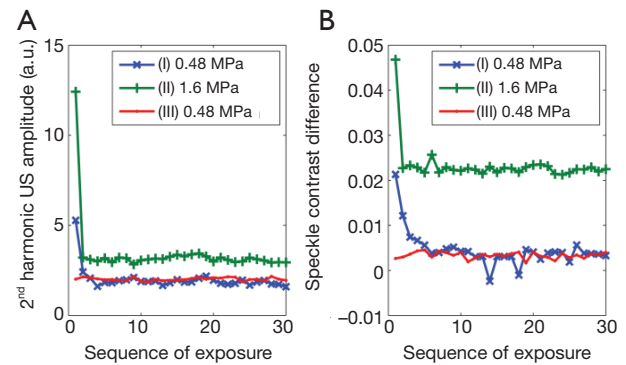


Figure 4 (A) Ultrasound signals with three groups of ultrasound exposures: 0.48, 1.6 and 0.48 MPa again; (B) simultaneously detected ultrasound modulated optical signals.

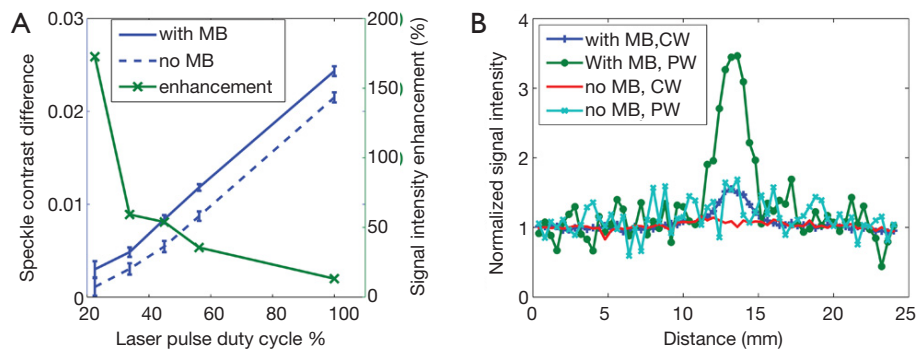


Figure 5 (A) Blue, comparison of speckle contrast difference between cases with and without microbubbles at different laser pulse duty cycles; green, contrast enhancement over laser pulse duty cycle in percentage; (B) line scan of the silicone tube with and without bubbles at CW and 34% duty cycle PW laser illumination. MB, microbubble; CW, continuous wave; PW, pulse wave.

measured with and without microbubbles divided by the signal without bubbles, is shown in (Figure 5A, green). It demonstrates that higher contrast improvement can be obtained using lower duty cycle laser pulses. This is because higher attenuation is applied to the fundamental frequency as shown in Figure 2D and therefore the effect of the non-linear oscillation of the microbubbles is enhanced.

Line scan images of the liquid filled silicone tube are shown in Figure 5B. Images with and without microbubbles using a CW laser and 34% duty cycle pulse wave (PW) laser are compared. Base lines of these images are normalized to 1 (each one-dimensional scan is divided by the mean of the first eight data points). Without microbubbles, the image of tube is hardly discernible in both CW and pulsed laser cases. With microbubbles and CW laser illumination, the image of the silicone tube can be observed while using pulsed laser illumination the contrast of the image is

significantly enhanced (~2 times).

Discussion

It has been demonstrated that the image contrast in USMOT can be enhanced through the use of microbubble contrast agents. Experimental results indicate that significant harmonic signal generation occurs when there are a high proportion of microbubbles present particularly in the event of microbubble destruction. In order to improve image contrast further, a pulse laser based speckle contrast detection technique was used to detect the harmonic ultrasound modulated signals. Compared with the pulse inversion technique (12), this speckle contrast detection is less efficient in separating the fundamental and second harmonic signals. However, this technique requires does not require phase stepping and therefore reduces the effects of speckle de-correlation which

is considerable in detecting microbubbles and also offers a high extend which is beneficial in USMOT. Depending on the duty cycle of the laser pulses the fundamental modulated optical signal can be attenuated by different amounts and this can be used to infer the effects of the higher harmonics. Although the fundamental signal is suppressed by the filter provided by the pulse sequence of the laser, the fundamental signal is still significant in this experiment. This means that oscillation due to the second harmonic detection is undetectable and transient signal detection due to destruction of the bubbles is dominant. In order to generate significant nonlinear signals the ultrasound pressure must be sufficient. In this work an ultrasound pressure of 480 kPa is used in the majority of the experiments and significant destruction of the microbubbles occurs. This was identified as being the dominant effect responsible for the generation of significant higher harmonic signals (*Figure 4*). Consequently, an approach similar to agent detection imaging (23) could also apply in this destruction regime. In this case, however, significant clearing of the microbubbles at the first frame is required as the contrast difference is calculated from the difference between the first frame and second frame. This appears to be the case in the measurements shown in *Figures 3* and *4*. The disadvantage of working at this regime is that microbubbles need to be replenished after each exposure although in practice this would occur naturally with microbubbles being transported in the blood stream. One further difficulty in using microbubbles in the experiment carried out in this work is that concentration and position of the microbubbles are dynamic parameters, due to Brownian motion, buoyancy and mechanical instability making it difficult to maintain the signal consistency during measurement. Future investigations studying the contrast enhancement that occurs in a regime where the nonlinear oscillations are consistent would enable improvement in the signal stability and repeatability. One of the possible ways this could be achieved is through the use of the pulse inversion technique (12) in which a short time interval is used between frames. In this case the fundamental signal can be significantly suppressed and the consistent second harmonic signal due to the use of lower ultrasound pressure would be dominant. Overall, the potential applications of microbubble enhanced USMOT lie in the measurement of blood oxygen saturation (16) and haemolysis monitoring (24).

Conclusions

The contrast enhancement in USMOT resulting from the

use of ultrasound microbubbles has been demonstrated. A pulsed laser based speckle contrast detection technique has been developed to attenuate the fundamental ultrasound modulated optical signals which is attributed to both target and background tissue. Destruction of the microbubbles was shown to be the dominant effect leading to contrast improvement as shown by simultaneously detecting the ultrasound and speckle contrast signals. Finally, line scans of a microbubble filled silicone tube embedded in a scattering phantom demonstrated experimentally the significant image contrast improvement that can be achieved using microbubbles and demonstrates the potential as a future clinical imaging tool.

Acknowledgements

This work was supported by the *Biotechnology and Biological Sciences Research Council (BBSRC) UK* (BB/F004826/1 and BB/F004923/1).

Disclosure: The authors declare no conflict of interest.

References

1. Li J, Ku G, Wang LV. Ultrasound-modulated optical tomography of biological tissue by use of contrast of laser speckles. *Appl Opt* 2002;41:6030-5.
2. L  v  que S, Boccara AC, Lebec M, Saint-Jalmes H. Ultrasonic tagging of photon paths in scattering media: parallel speckle modulation processing. *Opt Lett* 1999;24:181-3.
3. Murray TW, Sui L, Maguluri G, Roy RA, Nieva A, Blonigen F, DiMarzio CA. Detection of ultrasound-modulated photons in diffuse media using the photorefractive effect. *Opt Lett* 2004;29:2509-11.
4. Gross M, Goy P, Al-Koussa M. Shot-noise detection of ultrasound-tagged photons in ultrasound-modulated optical imaging. *Opt Lett* 2003;28:2482-4.
5. Ruan H, Mather ML, Morgan SP. Pulsed ultrasound modulated optical tomography with harmonic lock-in holography detection. *J Opt Soc Am A Opt Image Sci Vis* 2013;30:1409-16.
6. Xu X, Liu H, Wang LV. Time-reversed ultrasonically encoded optical focusing into scattering media. *Nat Photonics* 2011;5:154.
7. Wang YM, Judkewitz B, Dimarzio CA, Yang C. Deep-tissue focal fluorescence imaging with digitally time-reversed ultrasound-encoded light. *Nat Commun*

- 2012;3:928.
8. Si K, Fiolka R, Cui M. Fluorescence imaging beyond the ballistic regime by ultrasound pulse guided digital phase conjugation. *Nat Photonics* 2012;6:657-61.
 9. Zemp RJ, Kim C, Wang LV. Ultrasound-modulated optical tomography with intense acoustic bursts. *Appl Opt* 2007;46:1615-23.
 10. Li R, Elson DS, Dunsby C, Eckersley R, Tang MX. Effects of acoustic radiation force and shear waves for absorption and stiffness sensing in ultrasound modulated optical tomography. *Opt Express* 2011;19:7299-311.
 11. Selb J, Pottier L, Boccara AC. Nonlinear effects in acousto-optic imaging. *Opt Lett* 2002;27:918-20.
 12. Ruan H, Mather ML, Morgan SP. Pulse inversion ultrasound modulated optical tomography. *Opt Lett* 2012;37:1658-60.
 13. Ruan H, Mather ML, Morgan SP. Pulsed ultrasound modulated optical tomography utilizing the harmonic response of lock-in detection. *Appl Opt* 2013;52:4755-62.
 14. Frinking PJ, Bouakaz A, Kirkhorn J, Ten Cate FJ, de Jong N. Ultrasound contrast imaging: current and new potential methods. *Ultrasound Med Biol* 2000;26:965-75.
 15. Simpson DH, Chin CT, Burns PN. Pulse inversion Doppler: a new method for detecting nonlinear echoes from microbubble contrast agents. *IEEE Trans Ultrason Ferroelectr Freq Control* 1999;46:372-82.
 16. Honeysett JE, Stride E, Deng J, Leung TS. An algorithm for sensing venous oxygenation using ultrasound-modulated light enhanced by microbubbles. *Proc. SPIE* 8223, Photons Plus Ultrasound: Imaging and Sensing 2012, 82232Z (February 9, 2012); doi:10.1117/12.907952
 17. Yuan B, Liu Y, Mehl PM, Vignola J. Microbubble-enhanced ultrasound-modulated fluorescence in a turbid medium. *Appl Phys Lett* 2009;95:181113.
 18. Li J, Wang LV. Methods for parallel-detection-based ultrasound-modulated optical tomography. *Appl Opt* 2002;41:2079-84.
 19. Kirkpatrick SJ, Duncan DD, Wells-Gray EM. Detrimental effects of speckle-pixel size matching in laser speckle contrast imaging. *Opt Lett* 2008;33:2886-8.
 20. Miller DL, Averkiou MA, Brayman AA, Everbach EC, Holland CK, Wible JH Jr, Wu J. Bioeffects considerations for diagnostic ultrasound contrast agents. *J Ultrasound Med* 2008;27:611-32; quiz 633-6.
 21. Li J, Ku G, Wang LV. Ultrasound-modulated optical tomography of biological tissue by use of contrast of laser speckles. *Appl Opt* 2002;41:6030-5.
 22. Goodman JW. *Speckle phenomena in optics: theory and applications*. Roberts and Company (Greenwood Village), 2006.
 23. Youk JH, Kim CS, Lee JM. Contrast-enhanced agent detection imaging: value in the characterization of focal hepatic lesions. *J Ultrasound Med* 2003;22:897-910.
 24. Chen WS, Brayman AA, Matula TJ, Crum LA, Miller MW. The pulse length-dependence of inertial cavitation dose and hemolysis. *Ultrasound Med Biol* 2003;29:739-48.

Cite this article as: Ruan H, Mather ML, Morgan SP. Ultrasound modulated optical tomography contrast enhancement with non-linear oscillation of microbubbles. *Quant Imaging Med Surg* 2015;5(1):9-16. doi: 10.3978/j.issn.2223-4292.2014.11.30